A study of initial motion of soil aggregates in comparison with sand particles of various sizes

B. Raei[a], H. Asadi[b*], A. Moussavi[c], H. Ghadiri[d]

[a] *Msc Graduated Student, University of Guilan, Rasht, Iran,*

[b] *Department of Soil Science, Faculty of Agricultural Sciences, University of Guilan, Rasht, Iran,*

[c] *Department of Irrigation Eng., Faculty of Agricultural Sciences, University of Guilan, Rasht, Iran,*

[d] *Faculty of Environmental Sciences, Environmental Future Centre, Griffith University, Nathan, Queensland 4111,*

[*]Corresponding author:
Hossein Asadi
Department of Soil Science,
Faculty of Agricultural Sciences,
University of Guilan,
Rasht, Iran,
E-mail: asadi@guilan.ac.ir
Tel: +98 13 33690282
Fax: +98 13 33690281

Abstract

Critical shear stress and threshold stream power are two important soil characteristics controlling detachment of soil particles by runoff and have been used in process-based erosion models such as WEPP, GUEST and EUROSEM. In this research, laboratory experiments were conducted in a 20×350 cm flume to study the effects of particle size and density on initial motion. Two contrasting soil samples, a well-aggregated forest soil and a non-cohesive fluvial sand, were used to provide particles with different densities. Each sample was divided into six size classes. Flow bed in the flume was roughed according to testing area for each size class using a plate which sand particles from each size class were glued on it. The initial motion of the particles was determined by two methods. In the first method, slope was increased gradually for a given constant discharge until particles start to move from every point of the testing area. In the second method, flume slope was set to a given steepness and discharge was gradually increased until particles start to move. Three different discharges and three slopes were tested in the first and second methods, respectively. Each test replicated two times. Analysis of the data showed that the particle size and density and also their interaction significantly affect (P<0.001) critical shear stress and threshold stream power. The critical shear stress and threshold stream power increased with increasing particle size and density, but the impact of particle density is higher on the coarser particles than the finer ones. Threshold values measured for the sand particles were about 2.3 times of those measured for soil particles in the three coarser classes, this difference decreased to about 65 percent (1.65 times) in the three finer classes, and even the difference between the two types of particles was not significant for the finest class (0.125-0.053).

Key words: Modeling, Soil erosion, Particle density, Critical shear stress, Threshold stream power

1. Introduction

Soil erosion is a serious environmental problem threatening the future development of agriculture and society. The adverse influences of widespread soil erosion on soil health, agricultural production, water quality, and ecosystem well-being, have long been recognized as severe thread to human sustainability (Lal, 1998). It is not only a major factor responsible for the long-term degradation of land quality, but also a major non-point source for water pollution (Lei et al., 2008). Increased attention to these concerns has led not only to the adoption of improve measures for erosion control, but also to a better understanding of soil erosion mechanics and the development of more reliable erosion prediction tools (Lei et al., 2008).

Soil erosion consists of three processes of detachment or initiation of motion of soil particles, transport of detached particles, and deposition when sufficient energy is no longer available to transport the particles (Morgan, 2005). Knowledge of critical shear stress or threshold stream power is required for the prediction of soil erosion by physically-based soil erosion models (Moody et al., 2005). The force per unit wetted area that acts on a surface is defined as shear stress, τ, and is expressed as:

$$\tau=\rho g h S_f \quad (1)$$

where ρ is water mass density (kg m^{-3}), g is the gravity constant (m s^{-2}), h is the water depth (m) and S_f is the friction slope (degree) (Chow et al., 1988). Critical shear stress, τ_{cr}, occurs when the shear force exceeds the critical limit for soil detachment.

Detachment has also been related to stream power, Ω, in experimental studies (Merz and Bryan, 1993) as well as in modeling works (Rose et al., 1983a, 1983b; Hairsine and Rose,1992a, 1992b). Stream power is the product of shear stress and mean flow velocity, U (m s^{-1}):

$$\Omega=\rho g h S_f U \quad (2)$$

where Ω is stream power (W m^{-2}) (Chow et al., 1988). If S_f is assumed to be equal to S, Equation 2 can be written as follows:

$$\Omega=\rho g q S \quad (3)$$

where q is the volumetric flux per unit width (m^2 s^{-1}) and S is bed slope. Also in the case of stream power, Ω_0 is a threshold value below which no erosion occurs.

Critical shear stress can be related to the weight and angle of repose of particles, which depend on the particles size and form (Julien, 2010). Forces of adhesion strongly determine critical shear stress (Oliveira, 1997). This threshold stress is usually determined by extrapolation of a regression relationship between shear stress and transport rate or, in flume studies, by gradually increasing slope or water discharge rate until 'initial motion' of grains is first detected (James et al., 1990).

In the physically based soil erosion models it has been justified that the critical shear stress/threshold stream power is a bulk characteristic of the soil. However, some works indicate that in a mixture of different size particles, relatively larger particles/aggregates show less resistance to movement than the relatively smaller ones and are transported at a higher rate (Wiberg and Smith., 1985; Asadi et al., 2007, 2011; Shi et al., 2012; Wang et al., 2014). The reason for this behavior could be the presence of different transport mechanisms acting on different size classes, and/or greater resistance to movement (i.e. a higher critical shear stress) of relatively smaller particles. On the other hand, there is considerable discrepancy in the published results regarding the measurements of critical shear stress (i.e. Wilcock, 1988; Petit, 1990; Moody et al., 2005; Bohling, 2009; Araujo et al., 2008; Salehi and Storm, 2012). These discrepancies are not random, but fall into four groups that may be associated with (i) difficulty in defining the beginning of motion of soil particles, (ii) using

two broad classes of methods for determining initial motion, (iii) running the measurements under hydraulically different conditions, and (iv) using the cohesive or non-cohesive materials. There are also various theoretical equations (Wiberg and Smith 1985; James et al., 1990; Leonard and Richard, 2004; Matthieu and Belleudy, 2007; Julien, 2010) for predicting critical shear stress each developed for a certain situation or particular particles.

In the process of surface erosion of well aggregated soils especially under flow dominant condition (e.g. rill erosion), the particles are mainly transported as aggregates. It has also been observed that sediment size distribution is bimodal under steady flow (Asadi et al., 2007, 2011; Shi et al., 2012) and rainfall of various kinetic energies (Wang et al., 2014). On the other hand, the study of the initial motion of soil aggregates is very rare, and most of the studies have focus on sand particle and/or cohesive soils. Therefore, this study was aimed to evaluate the initial motion of soil aggregates of various sizes in comparison with sand particles of same size. The initial motion was measured by two methods. The angle of repose was also measured for both soil aggregates and sand particles. Finally, the applicability of the exiting theories for the critical shear stress of sand particles was tested for soil aggregates.

2. Material and method

2.1. Soil sample selection and preparation

Two contrasting soil materials were used in the study to provide particles with different densities. The first soil was a well aggregated forest soil (a Mollisols), and the second one was a non-cohesive fluvial sand. The forest soil has a clayey texture containing 5.25% and 2.75% organic matter and equivalent calcium carbonate, respectively. Secondary particle (aggregate) size distribution (denoted PSD) of the two samples as measured by wet sieving was almost similar. The soil aggregates were quiet stable in water. Each air-dried sample

was divided to six size classes of 0.053-0.125, 0.125-0.5, 0.5-1, 1-1.6, 1.6-2, 2-2.36 mm by dry sieving. The particle density of the fluvial sand particles was measured using hydrometer method, and the particle density of the forest soil particles (aggregates) was measured using method suggested by Chepil (1950) (Fig. 1).

2.2. Measuring the Angle of repose

In this study the angles of repose (AoR) of soil size classes were determined by sliding method (Geldart et al., 2006) (Fig. 2a). Soil samples were filled into a hollow container to the brim and were gently leveled with a brush. The sliding AoR was defined as the angle of rotation from horizontal plane to an angle when the particles began to slide. Angle of repose was determined for the six size classes of both soil and sand samples with two repeats. To determine the impact of container dimensions on angle of repose, the measurements were carried out in containers with seven different sizes. The dimensions of the containers were 8×4×2, 8×4×4, 8×4×6, 12×4×2, 16×4×2, 8×6×2 and 8×8×2 cm. Also the AoRs were measured in a 10 × 5 × 5 cm container which was similar to the test section of the flume used for determining critical shear stress (see section 2.3).

To evaluate the effect of container size, particle size, particle type (density) and their interaction on the AoR, the measured data were subjected to two-way analysis of variance (ANOVA) using the statistical analysis software, SPSS. Tukey's honestly significant difference (HSD) was used to determine differences in the particle size and soil type among container dimensions at $\alpha = 0.05$ level.

2.3. Experimental Flume and the preparation of stream bed

The critical shear stress for soil and sand samples were measured in a solid base tilting flume of 350 cm long (Fig. 2b) with runon facility made from clear plastic. The flume was 20 cm wide and 20 cm deep with a head box and diffuser at one end and open at the other

end. A polystyrene, bottom insert (20 cm wide, 5 cm thick and 190 cm long) was place on the floor of the flume with a test section (5 cm wide, 10 cm long, and 5 cm deep) cut in its center. This test section was located 130 cm downstream from the upper end of the polystyrene, and 50 cm upstream from the flume exit. The distance from the flume sidewalls of test area was 7.5 cm. The bed roughness of the flume was adjusted to be the same as the sample by plastic talc (20 cm wide by 5 cm thick and 190 cm long) fixed on the polystyrene surface. The top side of the plastic talc was glued with uniform sand particles of each size classes. Accordingly, six plastic talcs were prepared for the six size classes of 0.053-0.125, 0.125-0.5, 0.5-1.0, 1.0-1.6, 1.6-2, 2.0-2.36 mm (Fig. 2c). This specific setup was to ensure that (i) the flow is fully developed and in steady state condition on the test area (Rause, 1946; Ranga raju et al, 2000), (ii) the sidewall effect upon the measured shear stress at the center of the flume is negligible (Moody et al., 2005), and (iii) test section is sufficiently small for a more accurate evaluation of the initial motion of the particles (Lei et al, 2008). The samples were packed in the test section in three layers of 2, 2 and 1 cm. Each layer gently compacted using a piece of cubic wood. The last layer was very carefully leveled off with the fixed bed. The sample in the test area was saturated very slowly by a wash bottle two hours before each run.

2.4. Method of measuring the initiation of particle movement

The initiation particle motion from the test samples was determined by two methods. In the first method, flow was kept constant but flume slope was gradually increased until particles noticeably begin to move from the test section. Three different flow rates were tested and measurements of the flume slope at which particle movement began were repeated two times for each size class of the two samples. In the second method, the flume slope was kept constant but flow discharge slowly increased until the particles begin to move from the test samples. Three different flume slopes were tested and measurements of the flow discharge

at which particle movement began were repeated twice for each size class of the two samples. In all 144 runs were carried out for measuring the initiation movement of particles.

The criterion for the initiation of motion used in this study was the initiation of noticeable particle motion (Moody et al., 2005). This was defined to be the continuous movement of particles from every point of the testing area which was determined visually. Unlike the first visible particle motion, noticeable motion is independent of time and thus less ambiguous (Moody et al., 2005). It should be taken into consideration that with increasing flow rate or flume gradient, particularly when such increase is not at very small increments, small waves propagate in the flow that may bring some particles into motion. This can not be considered as the starting point of motion of particles and the critical shear stress (Moody and Smith, 2005). Accordingly, the initiation of particle motion was examined by visual observation 5 to 10 seconds after the increasing of flow rate or flume gradient (Moody et al., 2005). After calculating shear stress using eq. 1 with the assumption of S_f=S, critical shear stress on the horizontal surface was calculated with the following formula:

$$\tau_{cr} = \psi \, \tau_{cr,0} \tag{4}$$

$$\psi = \sin(\phi \pm \beta) / \sin\phi \tag{5}$$

where $\tau_{cr,0}$ is critical bed-shear stress on a horizontal bed, ψ correction coefficient of critical bed-shear stress for the longitudinal direction slopes, ϕ is angle of repose in degree (+ indicates an upsloping bed and "-" a downsloping bed) and β is longitudinal bed slope angle (Duan et al., 2001). Calculations were also carried out for threshold stream power using eq. 3. Table 1 shows the range of flow characteristics in the experiments.

To evaluate the effect of measurement method, particle size, particle type (density) and their interaction on the initiation movement of particles, the measured data on τ_{cr} and Ω_0 were

subjected to two-way analyses of variance (ANOVA) using the statistical analysis software, SPSS. Tukey's honestly significant difference (HSD) was used to determine differences in the mean values at $\alpha = 0.05$ level of significance.

3. Results and discussion

3.1. The angle of repose

The AoR clearly depends on particle size, soil type and container dimension. Table 2 shows the particle AoRs for two soil types and six particle size classes measured in containers of different dimensions. The results of ANOVA showed that the length, width and depth of the containers, and their interactions with particle size all significantly ($P<0.001$) affected AoR. whereas the AoR increased significantly with width and depth of the container, it decreased with container's length (Table. 2). It seems that the higher the ratio of the particle weight (amount) to cross section of container is, the smaller the resultant AOR becomes. Geldart et al. (1990) noted that there is no general agreement for the best design or size of equipment or the optimum amount of material to measure the angle of repose.

Since the AoR is significantly affected by the container dimension and no optimum container size could be found, we, therefore, used a container for all of our AoR measurements with the same dimensions as the test section of the flume used for measuring critical shear stress. The AoRs measured by this container also varied significantly ($P<0.001$) with soil type and particle size. No significant cross interaction is found between the particle type and size at $P > 0.05$. The average AoR of sand particles (49.8 degree) was significantly smaller than that of the forest soil particles (50.6 degree), suggesting that, the shape of the different particle types should be measured (perhaps using the Corey shape factor), and the data to be used to test the hypothesis that "this difference, though small, is related to density and shape".

The effect of particle size on AoR is significant (Fig. 3). Whereas the smallest size class 0.053-0.125 mm showed a high value of AoR (53.3^{o} and 55.3^{o} for soil and sand respectively), AoR decreased rapidly for the next size class to a minimum of 46.0^{o} and 46.8^{o} and then linearly increased with particle size for size classes of larger than 0.5 mm. In general, the formation of AoR is related to the resultant inter-particle forces, interaction force and the gravity force (Wang et al., 2010). When particles are small, the inter-particle forces become dominant so that the particles no longer behave as individuals but as a cohesive group. When the particles are large enough, the inter-particle forces no longer play a dominant role on the AoR, and the particles behaves as individuals and not as groups, therefore the effects of size and weight become dominant and the angle of repose increases with particle size (Yang et al., 2009; Wang et al., 2010).

3.2. Initiation of particle movement

3.2.1. Critical shear stress

Measured critical shear stress was found to be dependent on the soil type, particle size, and measurement method. Critical shear stress of sand particles was 2.15 times higher than that of soil particles (1.176 vs. 0.547 Pa). As disturbed samples were used for both materials with no compaction, the measurements carried out immediately after saturation, and the average angle of repose was almost the same for the two samples[1], the major reason for such a big difference in critical shear stress is due to particle density which affects particle weight. The average density of soil particles was 1.76 g cm^{-3} in comparison to 2.66 g cm^{-3} of sand particles. The ratio of submerged density (σ-ρ) of sand to soil particles is 2.18, very closed to 2.15. The effect of particle density (i.e. submerged weight) has been included in

[1] Though the mean AoR of the two particle types was significantly different, but the difference was less than 2 percent (Section 3.1).

most equations used by researchers to predict critical shear stress (e.g. Neill, 1967; Wiberg and Smith, 1985; Leonard and Rechard, 2004; Matthieu and Belleudy, 2007).

Critical shear stress measured by the method in which the slope was kept constant and discharge gradually increased was in average 22 percent higher than that measured by the method in which discharge was kept constant and the slope gradually increased. However the difference for the sand particles was lower than that for the soil particles (10 percent vs. 50 percent). In other word, whereas the critical shear stresses for both samples were affected by the measurement method, the differences between the soil samples were very much higher than between the sand samples. Different sizes of the particles were affected differently by the measurement method used (Fig. 4). Whereas there was no significant difference between critical shear stresses measured by the two methods for fine to medium size classes (0.125-0.50, 0.50-1.0, and 1.0-1.60 mm), the difference was significant for the finest and the two coarsest size classes.

The interactive effect of type and size of the particles on the critical shear stress is presented in Figure 5. The coarsest size class of sand particles (2.00-2.36 mm) and the finest size class of soil particles (0.053-0.125 mm) showed the highest and lowest critical shear stress values respectively. The effect of particle type (i.e. density) on the critical shear stress was significant for all of the size classes except the finest one. Whereas the critical shear stress was significantly different for all the size classes of sand, there was no significant difference between the two finest size classes of forest soil. In both cases, critical shear stress increased exponentially with size (R^2=0.994 and 0.991), though with different exponent of 1.092 vs. 0.869 for sand and soil particles, respectively.

Roberts et al., (1998) reported that the critical shear stress of finer particles (5 micrometer in diameter) was strongly dependent on particle size and bulk density whereas for the larger

particles (1350 micrometer in diameter) critical shear stress was strongly dependent only on particle size. The particle volume and consequently its weight is a third order function of size (i.e. volume of a sphere is proportion to r^3), therefore it is apparently interpretable that critical shear stress being strongly dependent on particle size for the larger particles in compare to the finer ones. But in fact, particle size and density combined as one effective property (i.e. submerged weight), and their effect on critical shear stress could not be interpreted individually. In our case for example, the difference between critical shear stresses of two types of particles increased by particle size (Fig. 5). The particle density was almost constant (varies between 2.64 to 2.67) for all sizes of sand particles, and decreased for soil particles by size reaching to an almost constant value for the medium to coarse sizes (Fig. 1). Accordingly, for the four size classes of 0.5-1.0, 1.0-1.6, 1.6-2.0 and 2.0-2.36 mm, whereas the size is the same for sand and soil particles and the density is constant for both, the difference between critical shear stresses increases by size. Therefore the rate of dependency of the critical shear stress to particle size is strongly dependent on particle density. In other words, the critical shear stress increased with increasing particle size and density, but the impact of particle density is higher on larger particles. The critical shear stress of sand particles was about 2.3 times that of soil particles in the three larger classes, decreasing to about 65 percent (1.65 times) in the three smaller classes. The difference in critical shear stress between the two types of particles was not significant for the smallest size class (0.125-0.053 mm). This interactive behavior could be explained by particle density and the angle of repose. Whereas the particle density of sand is almost constant (2.64-2.67 g cm^{-3}) for all size classes, it decreases with size (from 2.08 to 1.75 g cm^{-3}) for the soil particles (Fig 1). With the assumption of same shape, the ratio of submerged weight of sand to soil particles is calculated to be 2.19 and 1.54 for the coarsest (2.175 mm) and the finest (0.089 mm) size classes, respectively. Also the ratio of angle of repose of soil to sand

particles is 1.021 and 1.037 for the coarsest (2.175 mm) and the finest (0.089 mm) size classes, respectively. The ratio of resistance force against the flow for sand particles to that of soil particles decreases by the reduction in particle size, which can results in the reduction of the difference between critical shear stress for sand and soil particles with decreasing particle size.

3.2.2. Threshold stream power

Measured threshold stream power also was found to be dependent of the soil type, particle size, and measurement method. The mean comparison of particle type×particle size interaction on the threshold stream power is presented in Figure 6. Similar to critical shear stress, threshold stream power of sand and soil particles increased exponentially (R^2=0.987 and 0.988, respectively) with size. All the size classes of sand particles showed significantly higher threshold streampower than those of soil particles, but the finest class (0.053-0.125 mm). Unlike the critical shear stress, the difference between the two types of particles and the differences among size classes are higher than that could be explained mainly by particle density and the angle of repose. The threshold stream power of sand particles was about 3 times of that of soil particles in average. On the other hand, the ratio of threshold stream power of the coarsest to finest size was about 28 and 20 for sand and soil particles respectively, whereas the ratios of critical shear stresses were 10 and 6 respectively.

3.3. The curves of critical shear stress and threshold streampower

Figure 7 shows the Sheilds-type diagram for sand and soil particles of different sizes using all data sets. The distance between the points of sand and soil particles shows the difference between their critical shear stresses which increases with size (see Section 3.2.1). The figure also shows that for a given size class, detachment of particles (both sand and soil) occurs over a range of shear stresses. This is well known for sediment detachment under stream

flows (Allen, 1994). But this figure shows another difference between soil and sand, the detachment of soil aggregates occurs in a wider range than the sand particles.

The measured data also were compared to the general theory of Julien, (2010) as shown below:

$$\tau_{*c} \approx 0.3e^{-d_*/3} + 0.06\tan\varphi\left(1 - e^{-d_*/20}\right) \tag{11}$$

where

$$d_* = d_S\left(\frac{(G-1)g}{\upsilon_m^2}\right)^{1/3} \tag{12}$$

where, τ_{*c} is the critical values of the Shields parameter, d_* is dimensionless particle diameter, d_S is particle size (m), φ is angle of repose, G is specific gravity, g is gravitational acceleration (m s^{-2}), υ_m is kinematic viscosity (m^2 s^{-1}).

For sand particles, Fig. 8 shows good agreement (Nash-Sutcliffe efficiency coefficient, E_{NS} is 0.989) between measured and predicted critical shear stress especially for coarse particles, but for soil particles (Fig 8) there is an under-prediction of about 35 percent on average. The under-prediction is about 5 percent on average for sand particles. Existence of some types of cohesion among soil particles especially the smaller ones can be responsible for the under predictions.

As the critical shear stress affected by the measurement method (Table 3), the measured data also were compared to the theory for each method separately (Fig 9). For sand particles, Fig. 9a shows good agreement between measured and predicted critical shear stress, and the errors are distributed normally for both methods (Nash-Sutcliffe efficiency coefficient, E_{NS} is 0.961 and 0.967, respectively). For soil particles (Fig 9b) whereas the errors are almost normally distributed around line 1:1 for method-A, there is an under-prediction for all size classes for method-B.

Considering the stochastic behavior of particle motion, Fig. 10 shows the diagram of threshold streampower for sand and soil particles using all data sets. This diagram (Fig 10) shows that the stochastic behavior of motion depends on particle size and type, it is higher for coarser particles than finest one, and higher for sand than soil particles.

4. Conclusion

This study aimed at investigating the angle of repose and initiation motion of soil aggregates of various sizes in comparison with sand particles of same size. The soil aggregates provided from surface layer of a forest Mollisols were quite stable in water, and had an average density about 1.76 g cm^{-3}. The average density of sand particles was 2.66 g cm^{-3}. The angle of repose, measured by sliding method, remarkably changes with particle size, and was significantly lower for sand particles than soil particles. It was highest for the finest and coarsest size classes.

Similar to sand particles, the initiation motion of soil aggregates was also, in general, a function of particle size. Critical shear stresses measured by the two methods, keeping the flow rate constant and increasing the flume sloped gradually or vice versa, were different for both sand particles and soil aggregates, but the difference was very much lower for sand particles than for soil aggregates (10 percent vs. 50 percent in average). This means that for soil aggregates, the case of surface soil erosion events, the method used for determining critical shear stress could result in an over or under prediction about 50 percent. The coarser the particles were, the higher the difference between their critical shear stresses measured by the two methods became, and the higher were their standard deviation (in average; 0.300 for the coarsest vs. 0.036 for the finest) of their measured values.

Critical shear stress of sand particles was significantly higher than that of soil aggregates, the coarser the particles were, the higher was the difference between critical shear stresses of sand particles and soil aggregates. Our results have shown that the rate of dependency of

the critical shear stress to particle size is strongly influenced by particle density. In this study, the difference between critical shear stresses of sand particles and soil aggregates increased by particle size (Fig 5). The particle density was almost constant for all sizes of sand particles, and decreased for soil aggregates by size reaching to an almost constant value for the medium to coarse sizes (Fig 1). Whereas the mean size is the same and the density is constant for sand particles and soil aggregates of size classes of 0.5-1.0, 1.0-1.6, 1.6-2.0 and 2.0-2.36 mm, the difference between critical shear stresses increases by size. Therefore, the effects of particle size and density on critical shear stress could not be separately interpreted. The two properties are combine as one effective property of "submerged weight". The critical shear stress increased with increasing particle size and density, but the impact of particle density is higher on larger particles.

There was good agreement between critical shear stress predicted using theory of uniform beds under stream flows with the measured values for the sand particles, but the theory under-predicted the critical shear stress of soil aggregates. The separate comparison between measured critical shear stresses and the predicted ones for the two methods of measurement showed that for sand particles, the degree of agreement was not different and the errors were distributed normally for both methods, but for soil particles, whereas the errors were almost normally distributed around line 1:1 for method-A, there was an under-prediction for all size classes for method-B.

Under shallow flows over soil beds, previous works indicate that in a mixture of different size particles, relatively larger particles/aggregates show a higher transport rate than the relatively smaller ones. Considering the two possible reasons for this behavior, the results of current study emphasizes on the presence of different transport mechanisms acting on different size classes rather than the greater resistance to movement (i.e. a higher critical shear stress) of relatively smaller particles.

References

Allen, J.R.L., 1994. Fundamental properties of fluids and their relation to sediment transport processes, In: K. Pye (Eds.), Sediment Transport and Depositional Processes. Blackwell Scientific Publications, pp. 25–60.

Araujo, M.A.V.C., Teixeira, J.C.F., Teixeira, S.F.C.F., 2008. Application of laser anemometry for measuring critical bed shear stress of sediment core samples. J. Cont. Shelf Res. 28, 2718–2724.

Asadi, H., Moussavi, A., Ghadiri, H., Rose, C.W., 2011. Flow-driven soil erosion processes and the size selectivity of sediment. J. Hydrol. 406, 73–81.

Asadi, H., Ghadiri, H., Rose, C.W., Yu, B., Hussein, J., 2007. An investigation of flow-driven soil erosion processes at low streampowers. J. Hydrol. 342, 134–142.

Bohling, B. 2009. Measurements of threshold values for incipient motion of sediment particles with two different erosion devices. J. Marine Syst. 75, 330–335.

Chepil, W.S. 1950. Methods of estimating apparent density of discrete soil grains and aggregates. Soil Sci. 70, 351–362.

Chow, V., Maidment, D., Mays, L., 1988. Applied Hydrology, Water Resources and Environmental Engineering, McGraw-Hill, New York.

Duan, J.G., Wang, S.S.Y., Jia, Y., 2001. The applications of the enhanced CCHE2D model to study the alluvial channel migration processes. J. Hydraul. Res. 39, 1–12.

Geldart, D., Abdullah, E.C., Hassanpour, A., Nwoke, L.C., Wouters, I., 2006. Characterization of powder flowability using measurement of angle of repose. China Particul. 4, 104–107.

Geldart, D., Mallet, M.F., Rolfe, N., 1990. Assessing the flowability of powders using angle of repose. Powder Handl. Proc. 2, 341−346.

Hairsine, P.B., Rose, C.W., 1992 a. Modeling water erosion due to overland flow using physical principals, 1. Sheet flow. Water Resour. Res. 28, 237– 243.

1 Hairsine, P.B., Rose, C.W., 1992 b. Modeling water erosion due to overland flow using physical
2 principals, 2. Rill flow. Water Resour. Res. 28, 245–250.

3 James, W.K., William, E.D., Fujiko, I., Hiroshi, I., 1990. The variability of critical shear stress,
4 friction angle and grain protrusion in waterworked sediments. Sedimentol. 37, 647–672.

5 Julien, P.Y., 2010. Erosion and Sedimentation, Second ed. Cambridge University Press.

6 Lal, R., 1998. Soil erosion impact on agronomic productivity and environment quality. Crit. Review
7 Plant Sci. 4, 319–464.

8 Lei, T.W., Zhang, Q.W., Yan, L.J., Zhao, J., Pan, Y.H. 2008. A rational method for estimating
9 erodibility and critical shear stress of an eroding rill. Geoderma. 144, 628–633.

10 Leonard, J., Richard, G., 2004. Estimation of runoff critical shear stress for soil erosion from soil
11 shear strength. Catena. 57, 233–249.

12 Matthieu, D.L., Belleudy, P. 2007. Critical Shear Stress of Bimodal Sediment in Sand-ravel Rivers.
13 J. Hydraul. Eng. 133, 555–559.

14 Merz, W., Bryan, R., 1993. Critical conditions for rill initiation on sandy loam brunisols: laboratory
15 and field experiments in southern Ontario, Canada. Geoderma. 57, 357–385.

16 Moody, J.A., Smith, J.D., Ragan, B.W. 2005. Critical shear stress for erosion of cohesive soils
17 subjected to temperatures typical of wildfires. J. Geophys. Res. 110, F01004,
18 doi:10.1029/2004JF000141.

19 Morgan, R.P.C., 2005. Soil Erosion and Conservation, Third edition. Blackwell Publishing, Oxford,
20 UK. 303 pp.

21 Neill, C.R., 1967. Mean velocity criterion for scour of coarse uniform bed material. Proc. Int. Assoc.
22 Hydraul. Res. 3, 46–54.

23 Oliveira, R., 1997. Understanding adhesion: A means for preventing fouling. Exp. Therm. Fluid Sci.
24 14, 316–322.

1 Petit, F., 1990. Evaluation of grain shear stresses required to initiate movement of particles in natural
2 rivers. Earth Surf. Proc. Land. 15, 135–148.

3 Ranga Raju, K.G., Asawa, G.L., Mishra, H.K., 2000. Flow-establishment length in rectangular
4 channels and ducts. J. Hydraul. Eng. 126, 533–539.

5 Roberts, J., Jepsen, R., Gotthard, D., Lick, W., 1998. Effects of particle size and bulk density on
6 erosion of quartz particles. J. Hydraul. Eng., ASCE 124, 1261–1267.

7 Rose, C.W., Williams, J.R., Sander, G.C., Barry, D.A., 1983a. A mathematical model of soil erosion
8 and deposition processes: I. Theory for a plane land element. Soil Sci. Soc. Am. J. 47, 991–995.

9 Rose, C.W., Williams, J.R., Sander, G.C., Barry, D.A., 1983b. A mathematical model of soil erosion
10 and deposition processes: II. Application to data from and aride-zone catchement. Soil Sci. Soc.
11 Am. J. 47, 996–999.

12 Rouse, H., 1946. Elementary Mechanics of Fluids. Wiley, New York.

13 Salehi, M., Strom, K., 2012. Measurement of critical shear stress for mud mixtures in the San Jacinto
14 estuary under different wave and current combinations. J. Cont. Shelf Res. 47, 78–92.

15 Shi, Z. H., Fang, N. F., Wu, F. Z., Wang, L., Yue, B. J., Wu, G. L. 2012. Soil erosion processes and
16 sediment sorting associated with transport mechanisms on steep slopes. J. Hydrology, 454–455,
17 123–130.

18 Wang, L., Shi, Z.H., Wang, J., Fang, N.F., Wu, G.L., Zhang, H.Y., 2014. Rainfall kinetic energy
19 controlling erosion processes and sediment sorting on steep hillslopes: A case study of clay loam
20 soil from the Loess Plateau, China. J. Hydrol. 512, 168-176.

21 Wang, W., Zhang, J., Yang, S., Zhang, H., Yang, H., Yue, G., 2010. Experimental study on the angle
22 of repose of pulverized coal. Particuology 8, 482–485.

23 Wiberg, P.L., Smith, J.D., 1985. A theoretical model for saltating grains in water. J. Geophys. Res.
24 90, 7341–7354.

1 Wilcock, P.R., 1988. Methods for estimating the critical shear stress of individual fractions in
2 mixed-size sediment. Water Resour. Res. 24, 1127–1135.

3 Yang, F.G., Liu X.N., Yang K.J., CAO, S.Y. 2009. Study on the angle of repose of nonuniform
4 sediment. J. Hydrodyn. 21(5): 685-691.

5

Table 1
Click here to download Table: table 1.docx

Table 1. The characteristics of flow used in this study

Soil type	Size Class (mm)	Slope (%)		Discharge ($ml.s^{-1}$)		Depth (mm)		Reynolds number		$\tau_{cr,0}$ (Pa)		Ω_c ($W.m^{-2}$)		D/d (mm)	
		mean	sd	mean	sd	mean	sd	mean	sd	mean	sd	mean	sd	mean	sd
Sand	**0.053-0.125**	1.05	0.386	62.86	27.80	2.83	2.83	312	138	0.273	0.068	0.028	0.007	31.83	8.37
	0.125-0.5	1.38	0.697	93.07	35.05	3.28	3.27	462	174	0.396	0.111	0.052	0.009	10.48	2.64
	0.5-1	1.98	1.033	107.76	45.21	3.18	3.17	536	224	0.576	0.213	0.155	0.137	4.24	1.52
	1-1.6	2.21	1.093	262	93.70	6.05	6.04	1303	465	1.201	0.131	0.247	0.020	4.65	1.30
	1.6-2	2.87	1.431	356	149	8.85	8.84	1771	741	2.317	0.372	0.469	0.057	4.91	2.36
	2-2.36	4.11	0.989	509	121	8.08	8.07	2527	601	3.212	0.277	0.969	0.108	3.70	0.70
Soil	**0.053-0.125**	0.89	0.483	39	24.37	2.58	2.58	196	121	0.193	0.067	0.012	0.001	29.02	8.83
	0.125-0.5	0.870	0.511	57.74	36.27	3.03	3.02	287	180	0.219	0.089	0.017	0.003	9.68	2.81
	0.5-1	1.21	0.57	78.22	36.43	3.21	3.20	388	180	0.337	0.079	0.038	0.007	4.27	1.23
	1-1.6	1.31	0.63	166.79	77.33	5.14	5.13	828	383	0.564	0.351	0.084	0.016	3.95	1.32
	1.6-2	1.25	0.58	231.21	73.61	6.38	6.36	1148	365	0.742	0.277	0.134	0.046	3.54	0.80
	2-2.36	1.75	0.58	333.05	106.45	8.39	8.38	1654	528	1.339	0.281	0.258	0.062	3.85	0.99

Table 2

Click here to download Table: table 2.docx

Table 2. Angle of repose of six particle sizes and two soil types measured by containers with different dimensions (cm).

Container\particle size (mm)	0.053-0.125	0.125-0.5	0.5-1	1-1.6	1.6-2.0	2.0-2.36	mean
Sand: Changing length							
2×4×8	50.2	45.8	46.1	47.6	49.0	50.2	**48.1**
2×4×12	52.8	45.3	46.5	47.2	48.2	48.7	**48.1**
2×4×16	47.3	43.2	42.6	44.9	45.0	46.5	**44.9**
mean	**50.1**	**44.8**	**45.0**	**46.5**	**47.4**	**48.5**	
Changing width							
2×4×8	50.2	45.8	46.1	47.6	49.0	50.2	**48.1**
2×6×8	49.6	45.5	46.5	47.6	48.7	49.0	**47.8**
2×8×8	52.1	45.2	46.4	48.9	50.3	51.8	**49.1**
mean	**50.6**	**45.5**	**46.3**	**48.0**	**49.4**	**50.3**	
Changing depth							
2×4×8	50.2	45.8	46.1	47.6	49.0	50.2	**48.1**
4×4×8	48.8	45.0	46.3	47.4	48.0	48.7	**47.4**
6×4×8	52.6	48.4	47.0	50.1	51.2	53.0	**50.4**
mean	**50.5**	**46.4**	**46.5**	**48.3**	**49.4**	**50.6**	
Soil: Changing length							
2×4×8	55.5	47.2	46.6	47.6	49.5	52.4	**49.8**
2×4×12	56.4	46.2	46.8	48.4	49.2	49.2	**49.4**
2×4×16	56.0	46.7	43.6	46.2	46.7	47.7	**47.8**
mean	**56.0**	**46.7**	**45.6**	**47.4**	**48.48**	**49.75**	
Changing width							
2×4×8	55.5	47.2	46.6	47.6	49.5	52.4	**49.8**
2×6×8	56.4	46.8	46.2	46.4	49.7	49.8	**49.2**
2×8×8	56.6	47.7	47.7	50.6	51.9	53.2	**51.3**
mean	**56.2**	**46.9**	**46.8**	**48.2**	**50.3**	**51.8**	
Changing depth							
2×4×8	55.5	47.2	46.6	47.6	49.5	52.4	**49.8**
4×4×8	48.9	46.6	45.0	48.7	48.8	50.6	**48.1**
6×4×8	53.0	48.4	47.6	48.7	52.8	54.0	**50.7**
mean	**52.5**	**47.4**	**46.4**	**48.3**	**50.4**	**52.3**	
Container*: 5×5×10							
Soil	53.3	46.8	46.0	48.4	51.0	53.4	**49.8**
Sand	55.3	47.2	46.8	48.4	51.3	54.5	**50.6**

* This container has the same dimension as the test section of the flume used for measuring critical shear stress

Figure

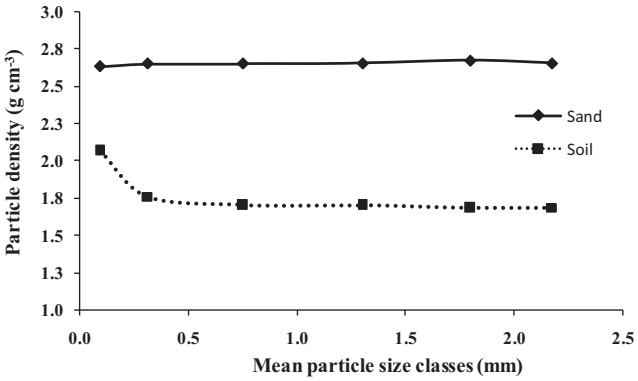

Figure 1. Particle density of sand and soil size classes

Figure 2

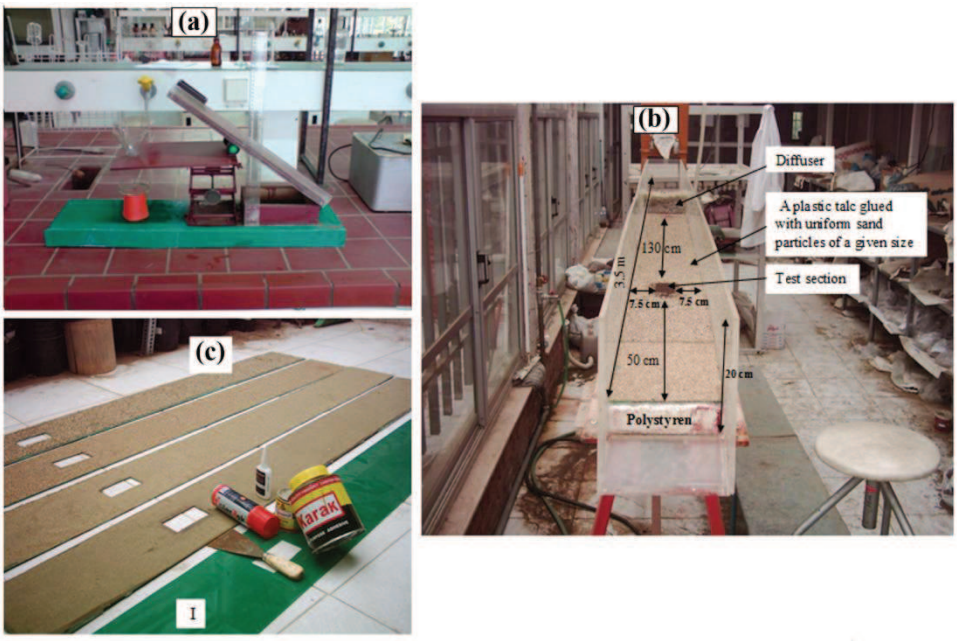

Figure 2- a) Device for measuring the angle of repose, and b) Flume channel after inserting plastic talc specified roughness, c) The plastic talcs which uniformly glued by classified sand particles (the talc I is without glued sand and the others are glued by different sand classes)

Figure 3

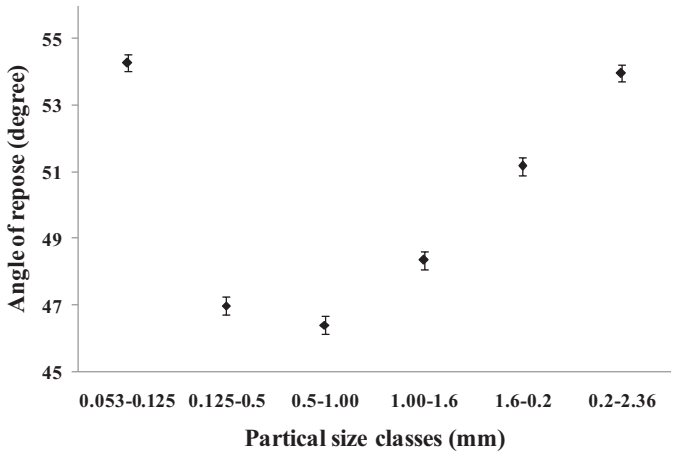

Figure 3. The effect of particle size on the angle of repose (measured by container with dimensions 5×5×10 cm).

Figure 4

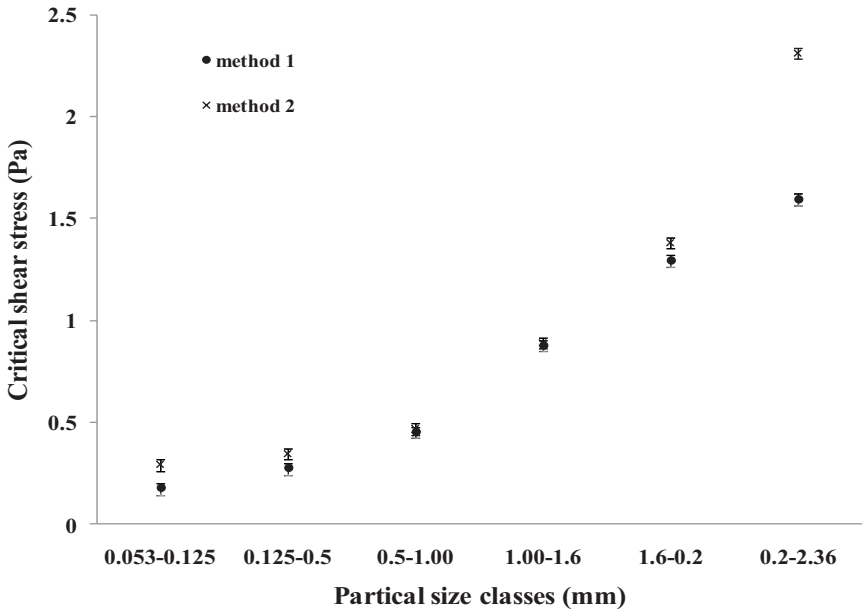

Figure 4. The interactive effect of measurement method and particle size on critical shear stress.

Figure 5

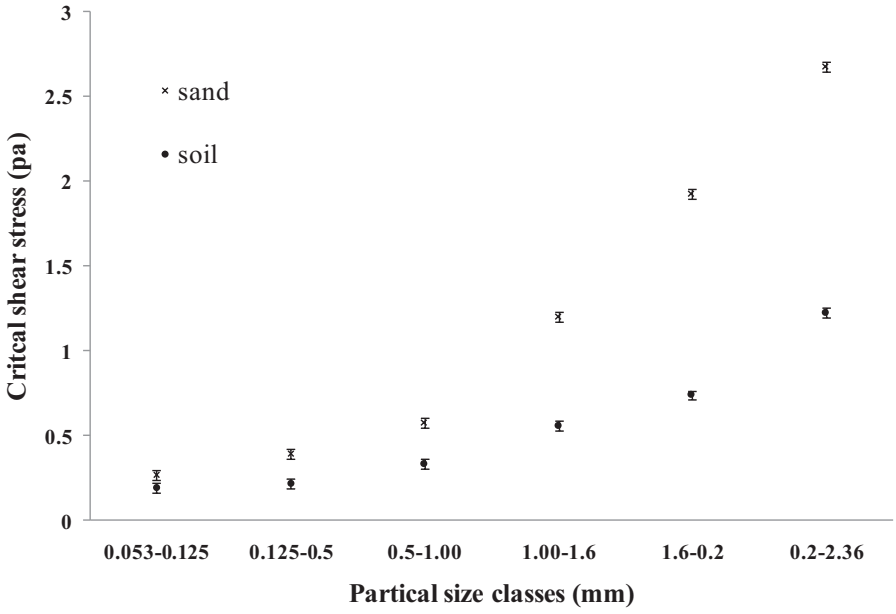

Figure 5. The interactive effect of soil type and particle size on critical shear stress.

Figure 6

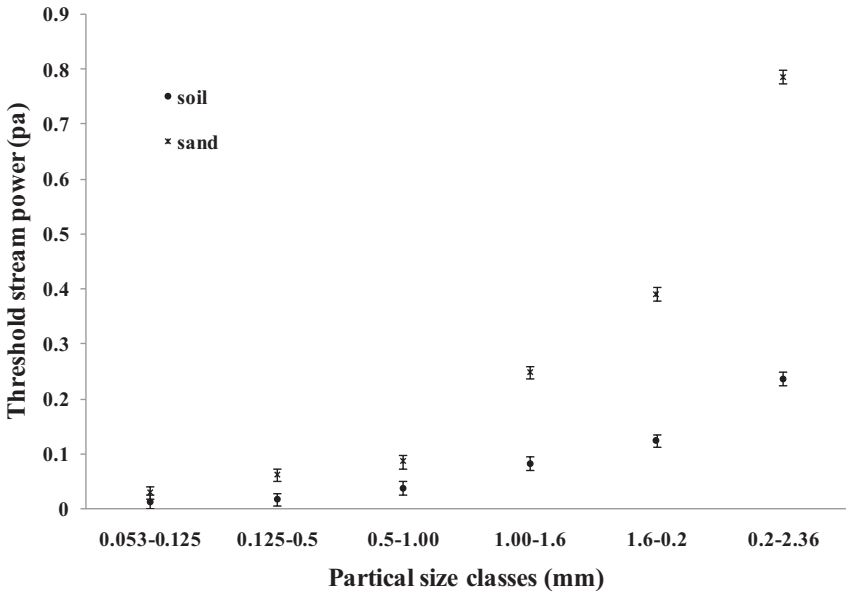

Figure 6. The effect of particle size and soil type on threshold stream power.

Figure 7

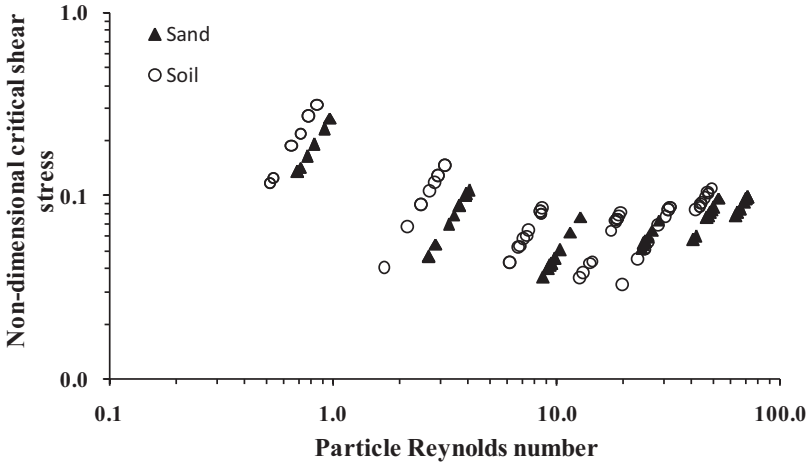

Figure 7. The Sheilds-type diagram for sand particles and soil aggregates.

Figure 8

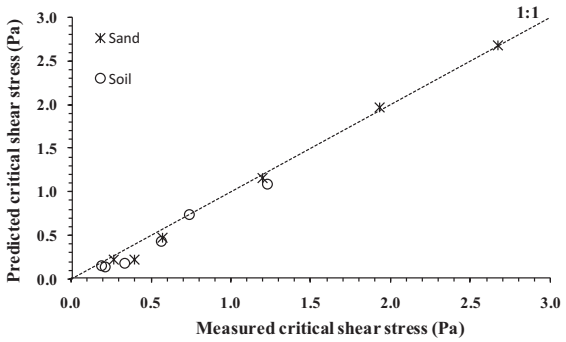

Figure 8. Comparison of measured critical shear stresses (mean values) with their predicted ones using Eqn. (11) for the sand particles and soil aggregates.

Figure 9

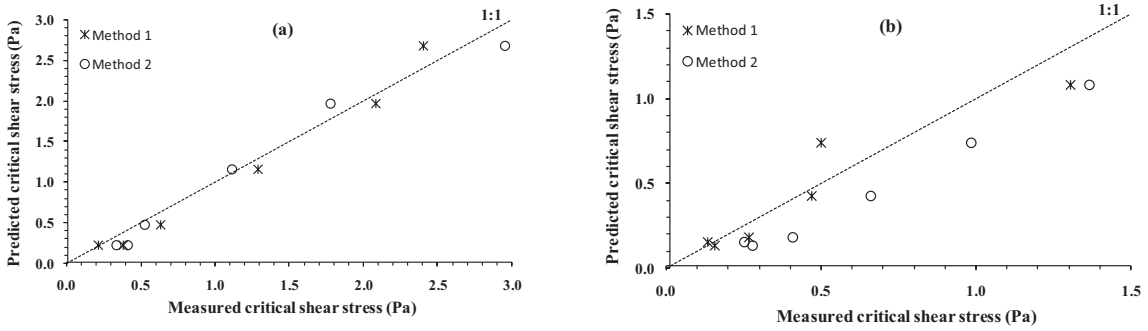

Figure 9. Comparison of measured critical shear stresses using two methods with their predicted ones for the sand (a) and soil (b) particles.

Figure 10

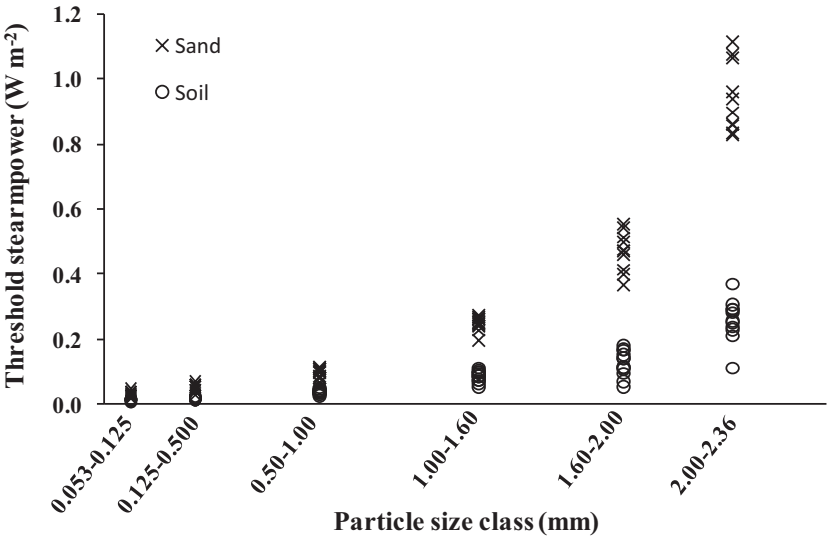

Figure 10. The threshold stream power for different size classes of sand particles and soil aggregates.